Biochemical and Biophysical Research Communications 463 (2015) 297–302

Contents lists available at ScienceDirect

Biochemical and Biophysical Research Communications

journal homepage: www.elsevier.com/locate/ybbrc

Crystal structure of the death effector domains of caspase-8

Chen Shen [a], Hong Yue [a], Jianwen Pei [a], Xiaomin Guo [a], Tao Wang [b, *], Jun-Min Quan [a, *]

[a] Key Laboratory of Structural Biology, School of Chemical Biology & Biotechnology, Peking University, Shenzhen Graduate School, Shenzhen 518055, China
[b] Laboratory for Computational Chemistry & Drug Design, School of Chemical Biology & Biotechnology, Peking University, Shenzhen Graduate School, Shenzhen 518055, China

ARTICLE INFO

Article history:
Received 4 May 2015
Available online 20 May 2015

Keywords:
Caspase-8
Death effector domain
Apoptosis
Necroptosis
Inflammation

ABSTRACT

Caspase-8 is a key mediator in various biological processes such as apoptosis, necroptosis, inflammation, T/B cells activation, and cell motility. Caspase-8 is characterized by the N-terminal tandem death effector domains (DEDs) and the C-terminal catalytic protease domain. The DEDs mediate diverse functions of caspase-8 through homotypic interactions of the DEDs between caspase-8 and its partner proteins. Here, we report the first crystal structure of the DEDs of caspase-8. The overall structure of the DEDs of caspase-8 is similar to that of the DEDs of vFLIP MC159, which is composed of two tandem death effector domains that closely associate with each other in a head-to-tail manner. Structural analysis reveals distinct differences in the region connecting helices α2b and α4b in the second DED of the DEDs between caspase-8 and MC159, in which the helix α3b in MC159 is replaced by a loop in caspase-8. Moreover, the different amino acids in this region might confer the distinct features of solubility and aggregation for the DEDs of caspase-8 and MC159.

1. Introduction

Caspase-8 is the major apical caspase that initiates apoptosis through the extrinsic pathway, and has also been shown to play key roles in several non-apoptotic processes such as necroptosis, inflammation, innate immunity, and cell migration [1–7]. Caspase-8 is characterized by the N-terminal prodomain and the C-terminal catalytic protease domain [8]. The C-terminal catalytic protease domain has been extensively studied and characterized by the determined structures of the apo protease domain or the complex of the protease domain in complex with peptide inhibitors or cellular FLICE-inhibitory protein (c-FLIP$_L$) [9,10]. The active protease domain is composed of a heterotetramer with two large and two small subunits [11]. However, the structural study of the N-terminal prodomain is hampered by its strong aggregating tendency and low solubility [12].

The N-terminal prodomain of caspase-8 is composed of two tandem death effector domains (DEDs) that belong to the death domain (DD) superfamily [13–15], which mediates the homotypic interaction with its partner proteins such as Fas associated death domain protein (FADD) in the death-inducing signaling complex (DISC) [16,17], or mediates the self-assembly in the death effector filaments [18,19]. No determined structure is currently available for the DEDs of caspase-8. The crystal structure of the soluble DEDs of vFLIP MC159 is generally used as a model to understand the homotypic interactions mediated by the DEDs of caspase-8 [20,21]. However, considering the low sequence homology (about 22%) and the distinct difference in solubility and aggregation between the DEDs of caspase-8 and MC159, the homology modeling might not be enough to characterize the full structural features of the DEDs of caspase-8. To address this problem, we determined the crystal structure of the tandem DEDs of caspase-8 at 2.2 Å resolution, which provides new insight into understanding the structure and functions of the DEDs of caspase-8.

2. Material and methods

2.1. Protein expression and purification

All clones were generated with a standard PCR-based cloning strategy, and the individual clones were verified by DNA sequencing. For biochemical assays and crystallization, the DEDs of human caspase-8 (residues 1–188) were subcloned into a pET-28a vector with N-terminal His6 or His-SUMO tags. The relevant mutants of Caspase-8 DEDs (residues1-188) were introduced by Fast

* Corresponding authors.
E-mail addresses: tau@pku.edu.cn (T. Wang), quanjm@pkusz.edu.cn (J.-M. Quan).

http://dx.doi.org/10.1016/j.bbrc.2015.05.054
0006-291X/

Mutagenesis System (*TransGen Biotech*). All the Caspase-8 DEDs constructs mentioned above were transformed into Rosetta (DE3) pLysS cells (Novagen). All recombinant protein expression was induced with 0.1 mM IPTG at 20 °C overnight. His-tagged proteins were purified with Qiagen Ni-NTA agarose according to the manufacturer's instructions. For crystallization, the His-SUMO tag was digested with Ulp1 overnight. The digestion was reloaded onto Ni-NTA resin. The flow-through was collected and concentrated to load on a Hiload 16/60 superdex 200 column (GE) to fractionate homogeneous DED proteins. The final purified DED protein was concentrated to 15 mg/ml in buffer A, composed of 20 mM Tris, pH 8.0, 1 mM DTT and 150 mM sodium chloride, and used for crystallization.

2.2. Crystallization and structure determination

The final purified caspase-8 DEDs (residues1-188, F122A/I128D) protein was concentrated to 15 mg/ml in buffer A, crystals were initially obtained as small needle clusters using the sitting-drop vapor diffusion method in reservoir buffer that contained 200 mM sodium chloride, 100 mM Tris, pH 8.5, 25% PEG3350. Crystals were optimized using hanging drop vapor diffusion method in reservoir buffer containing 160 mM sodium chloride, 80 mM Tris, pH 8.5, 20% PEG3350. After crystal screening, the diffraction data was collected in homesource Rigaku micromax-002+. Structure was solved by molecular replacement using the phaser-PHENIX software [22,23], using the crystal structure of the tandem DEDs of vFLIP MC159 (PDB code 2BBR) [20] as the initial search model. The final models were manually built in Coot [24] and refined by Refmac in CCP4 software [25,26]. The refinement statistics are shown in Table 1. The protein in the figures was rendered with PyMol [27].

2.3. Analytical size-exclusion chromatography

Analytical size-exclusion chromatography was performed on an AKTA FPLC system (GE Healthcare). Caspase-8 DED mutant proteins were loaded on to superdex 200 10/300 GL column (GE Healthcare) equilibrated with a buffer containing 20 mM Tris (pH 8.0), 500 mM NaCl, 1 mM DTT. The eluent was monitored by ultraviolet absorbance at 280 nm.

3. Results and discussion

3.1. Soluble mutants of the death effector domains of caspase-8

Over-expression of the wild-type tandem DEDs of caspase-8 in *Escherichia coli* remains a challenge due to the high aggregation and low solubility. On the other hand, the tandem DEDs of MC159 is soluble and retains the monomeric state in solution, which renders it easier to be characterized by biochemical and biophysical methods. To obtain soluble mutants of the DEDs of caspase-8, we performed a sequence alignment between the DEDs of caspase-8 and MC159, and also performed detailed structural analysis of the crystal structures of MC159 [20,21] to identify the potential residues that might affect the solubility of the DEDs of caspase-8. We found that several solvent-exposed and hydrophobic residues including Leu27, Met43 and Ile128 in caspase-8 are markedly distinct from the corresponding hydrophilic residues in MC159 including His33, Gln44 and Asn123, respectively (Fig. 1A).

To evaluate the influence of these residues on the solubility of caspase-8, three mutants L27H, M43Q, and I128N the DEDs of caspase-8 (residues 1–188) were constructed and overexpressed in *E. coli*. Fortunately, the expression showed that the mutant I128N was efficiently expressed and soluble in aqueous solution (Fig. 1B), but the purified protein precipitated while kept at 4 °C overnight after elution. We then mutated Ile128 to negatively charged aspartic acid, and the generated mutant I128D became more stable after elution. We could obtain root-like microcrystals at the concentration of 2 mg/ml after several rounds of crystallization screening (Fig. 1C), but the protein also precipitated when further concentrated. Inspired by the previous report that the F25Y mutation significantly improved the solubility of FADD [28,29], we thus mutated the corresponding solvent-exposed hydrophobic F122 on DED2 to alanine on the basis of the I128D mutant. The F122A/I128D mutant is highly homogenous and stable in aqueous solution under the concentration up to 15 mg/ml. Finally, we obtained rod-like crystals qualified for data collection after crystallization screening and optimization (Fig. 1D).

Table 1
Data collection and refinement statistics (molecular replacement).

PBD ID	4ZBW
Data collection	
Wavelength (Å)	1.5418
Space group	P1
Cell dimensions	
a, *b*, *c* (Å)	51.36, 52.11, 56.60
α, *β*, *γ* (°)	113.34, 116.89, 90.12
Resolution (Å)	2.20 (2.28–2.20)[a]
Total reflections	41,944
R_{merge}	0.052 (0.238)[a]
$I/\sigma I$	8.76 (2.59)[a]
Completeness (%)	96.6 (93.8)[a]
Redundancy	1.83 (1.59)[a]
Refinement	
Resolution (Å)	29.22–2.20
Unique reflections	22,971
R_{work}/R_{free}	0.204/0.251
No. atoms	3298
Protein	3050
Ligand/Ion	
Water	248
Average B factors	43.1
r.m.s. deviations	
Bond lengths (Å)	0.004
Bond angles (°)	0.810
Ramachandran statistics	
Most Favored (%)	98.0
Allowed (%)	2.0
Outlier (%)	0

Equations defining various *R* values are standard and hence are no longer defined in the footnotes.
[a] Values in parentheses are for highest-resolution shell.

3.2. Overall structure of the death effector domains$_{1\text{-}188}$

The crystal structure of the DEDs of the F122A/I128D mutant of caspase-8 (hereafter referred to as Casp8$^{F122A/I128D}$ unless otherwise specified) was determined by molecular replacement using the crystal structure of MC159 (PDB code 2BBR) [20] as the template, which was solved at 2.2 Å in the P1 space group with a dimer in the asymmetric unit (Fig. 2A and Table 1). The structure of DEDs contains residues 2–184, residues at the two extreme terminuses were not observed in the solved crystal structure.

The DEDs of Casp8$^{F122A/I128D}$ are composed of two tandem DEDs (DED1 and DED2) that have all α helical fold, which are closely associated with each other to form a dumbbell-shaped structure (Fig. 2B). The intramolecular interface between DED1 and DED2 is mainly formed by the hydrophobic residues from the helices α2a

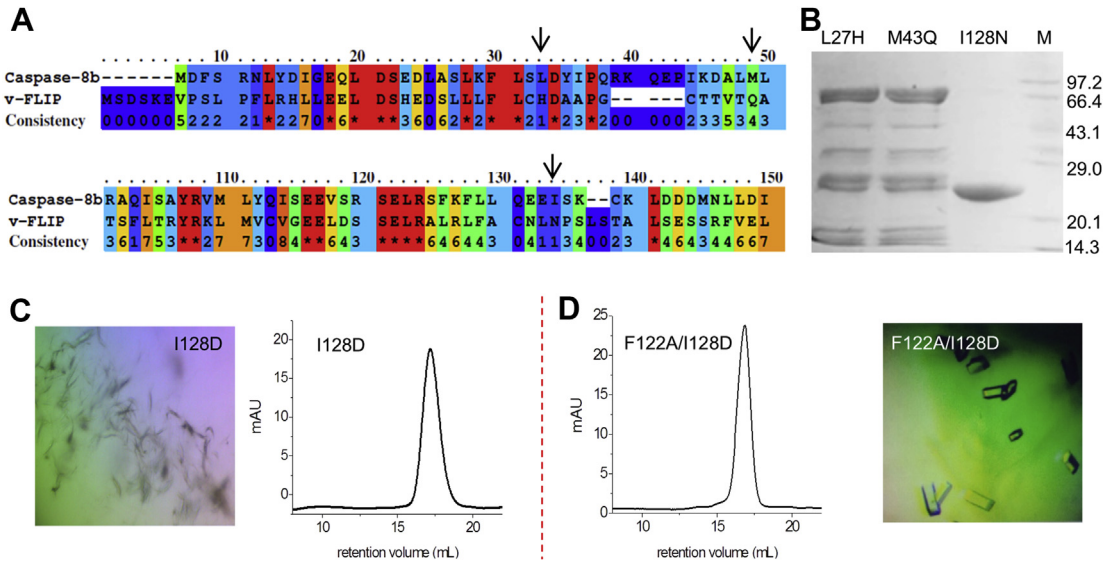

Fig. 1. Soluble mutants of the DEDs of caspase-8. A) Sequence alignment of the DEDs of casapse-8 and vFLIP MC159. Arrows denote the distinct residues between caspase-8 and vFLIP MC159. B) Expression of three solubility-modified mutants of the DEDs of caspase-8. The purity of the expressed protein is estimated by SDS–PAGE. C) Gel filtration and crystallization screening of the I128D mutant, the concentration limit of the protein is 2 mg/ml. D) Gel filtration and crystallization screening of the F122A/I128D mutant, the concentration limit of the protein is more than 15 mg/ml.

and α5a of DED1 and the helices α1b and α4b of DED2, and additionally strengthened by a peripheral hydrogen bonding network formed by Asp28, Ser99 and Arg102 from the C-terminus of helix α2a and the N-terminus of helix α1b, respectively (Fig. 2C). The overall surface of the DEDs of Casp8$^{F122A/I128D}$ is mainly characterized by charged residues except for a short hydrophobic patch at helix α2b of DED2 (Fig. 2D). Because both Phe122 and Ile128 locate at the surface of the protein, we could suppose that the overall structure of the DEDs of wild-type caspase-8 is at least highly similar to that of Casp8$^{F122A/I128D}$.

3.3. Structural comparison between the DEDs of caspase-8 and MC159

The overall structure of the DEDs of Casp8$^{F122A/I128D}$ is similar to that of the DEDs of MC159 with a root mean squared deviation of 1.25 Å for 122 equivalent Cα atoms between them despite their low sequence homology (about 22%) (Fig. 3A), highlighting the structural conservation for the death effector domain subfamily. On the other hand, the distinct functions and properties between the DEDs of caspase-8 and MC159 might be determined by the structural

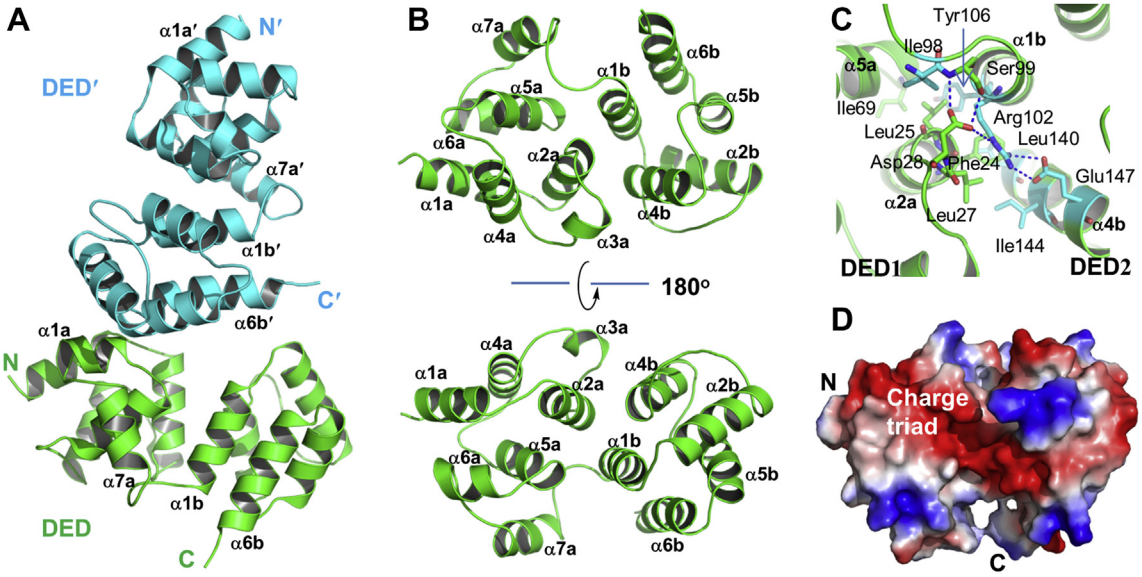

Fig. 2. Overall structure of the DEDs of Casp8$^{F122A/I128D}$. A) The dimeric structure of the DEDs of Casp8$^{F122A/I128D}$ in one asymmetric unit. B) Cartoon representation of the structures of the DEDs of Casp8$^{F122A/I128D}$ (residue 2–184). The helices in DED1 and DED2 are labeled by the helical number with a and b, respectively. C) The intramolecular interface between the two tandem DEDs of Casp8$^{F122A/I128D}$. The interfacial residues are shown by stick representations, hydrogen bonds are indicated by blue dashed lines in all figures. D) Electrostatic surface representation of the DEDs of Casp8$^{F122A/I128D}$, which is related to the structure of the lower panel in (B). (For interpretation of the references to color in this figure legend, the reader is referred to the web version of this article.)

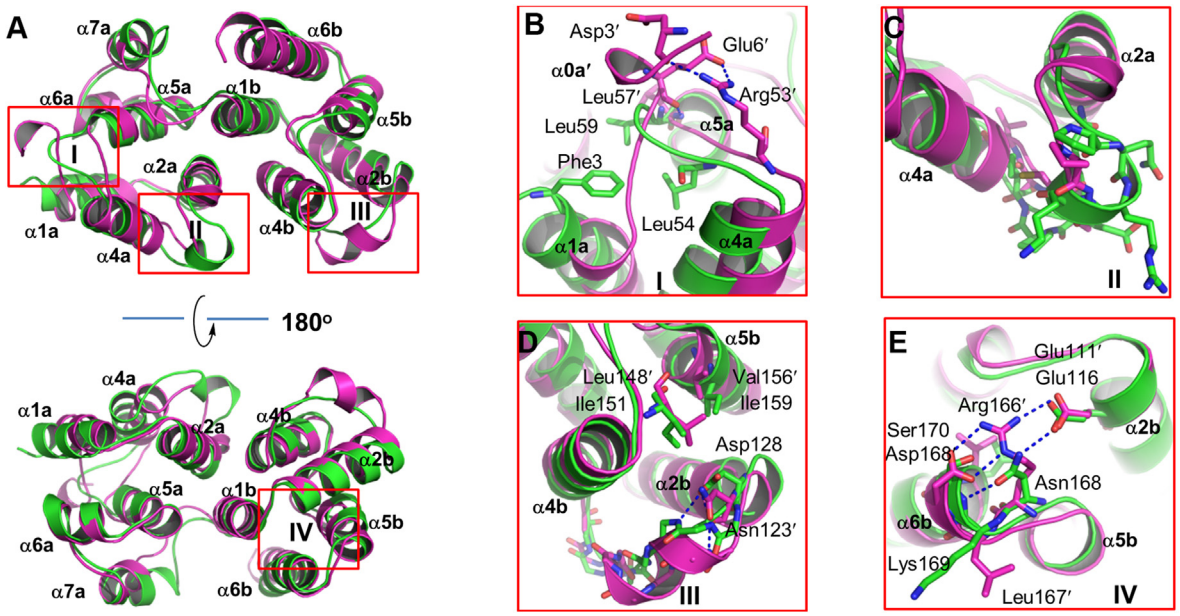

Fig. 3. Structural comparison of the DEDs of Casp8$^{F122A/I128D}$ and MC159. A) Superposition of the structures of the DEDs of Casp8$^{F122A/I128D}$ (green) and MC159 (magenta) (PDB code 2BBR) [20]. The four distinct regions are labeled by red solid line rectangles. B) Close view of the first distinct region that covers the N-terminus and the connecting loop between helices α4a and α5a. C) Close view of the second distinct region that connecting helices α2a and α4a in DED1. (D) Close view of the third distinct region that connecting helices α2b and α4b in DED2. (E) Close view of the fourth distinct region that involves the conserved E/D-RxDL motif. For all close views, the key residues in the highlighted regions are shown in stick representations, and numbered according to their individual sequences. The residues of MC159 are indicated with a prime. (For interpretation of the references to color in this figure legend, the reader is referred to the web version of this article.)

difference between these two proteins. The major structural variations locate at four regions as shown in Fig. 3A–E.

The first structural difference locates at the region including the extreme N-terminus and the connecting loop between helices α4a and α5a (Fig. 3B). The DED1 of MC159 is characterized by a short N-terminal extended helix α0a composed of a hydrophilic motif S^{2}DSKE^{6}. This motif forms hydrogen bonds with the connecting loop between helices α4a and α5a, which might stabilize the interactions between helices α1a, α4a and α5a. The N-terminal extended helix α0a is missing in the DED1 of Casp8$^{F122A/I128D}$, while the interactions between helices α1a, α4a and α5a are alternatively stabilized by the hydrophobic interactions between the N-terminal Phe3 of α1a and Leu54 and Leu59 from the longer connecting loop between α4a and α5a.

The second structural difference locates at the loop region connecting helices α2a and α4a (Fig. 3C). The short loop connecting helices α2a and α4a in DED1 of MC159 is replaced by a single turn helix in DED1 of Casp8$^{F122A/I128D}$. More strikingly, the surface of the helix is covered by multiple charged residues, which is similar to that of the DED of FADD [28,29].

The third structural difference locates at the connecting region between helices α2b and α4b (Fig. 3D). The helix α3b in MC159 is replaced by a loop connecting helices α2b and α4b of DED2 of Casp8$^{F122A/I128D}$. Notably, the mutation I128D that markedly improves the solubility of the DEDs of caspase-8 just locates at the beginning of the connecting loop, and the corresponding residue Asn123 in MC159 locates at the similar position, highlighting that the residues in this region might confer the solubility of the DEDs. According to the determined structure, Ile128 in the wild-type DEDs of caspase-8 should form a tight hydrophobic core with the spatially neighboring hydrophobic residues Ile151 at helix α4b and Ile159 at helix α5b. In this regard, the mutations I128N or I128D might improve the solubility of the DEDs partially through disrupting the hydrophobic interactions in this region.

The fourth structural difference locates at the region characterized by the conserved E/D-RxDL motif on helices α2b and α6b in DED2 of MC159, while RxDL is replaced by NxSL in DED2 of Casp8$^{F122A/I128D}$ (Fig. 3E). The E/D-RxDL motif in MC159 forms extensive hydrogen bonding interactions, and the hydrogen bonding interactions are relatively less prominent formed by the E-NxSL motif in DED2 of Casp8$^{F122A/I128D}$. However, both hydrogen bonding networks would play similar role in maintaining the structural integrity of this region.

3.4. Crystal packing of the death effector domains

The crystal structure of the DEDs of Casp8$^{F122A/I128D}$ was solved as a dimer in the asymmetric unit (Figs. 2A and 4A), in which two molecules pack perpendicularly in a head-to-tail manner. The dimeric interface is characterized by two hydrogen bonding networks (Fig. 4B). One is formed between Arg82 at the loop connecting helices α6a and α7a of DED1 from one monomer and Glu126 at helix α2b and Gln166 at helix α5b of DED2 from another monomer. Intriguingly, another one is formed between the conserved E/D^{18}-R^{71}xDL motif in DED1 from one monomer and Lys169 of the E-Nx^{169}SL motif in DED2 from another monomer, in which the positively charged Lys169 is surrounded by three continuing negatively charged residues including Asp15, Glu17 and Asp18, and the backbone amide of Lys169 forms an additional hydrogen bond with Asp73. This hydrogen bonding network might shed new light on understanding the functions of the E/D-RxDL motif in the homotypic interactions for the death effector domains [20,30].

Further analysis of the packing in the crystal lattice revealed a filamentous structure formed by the repeated DEDs in a head-to-tail manner through the dimeric interface (Fig. 4C). Given that the condition used for protein crystallization has been considered as a good approximation of overexpression of protein in the crowed environment of the cell [31], the dimeric interface possibly mediates the formation of death effector filaments upon overexpression of the DEDs of caspase-8 in cells [18,19]. Notably, positively charged

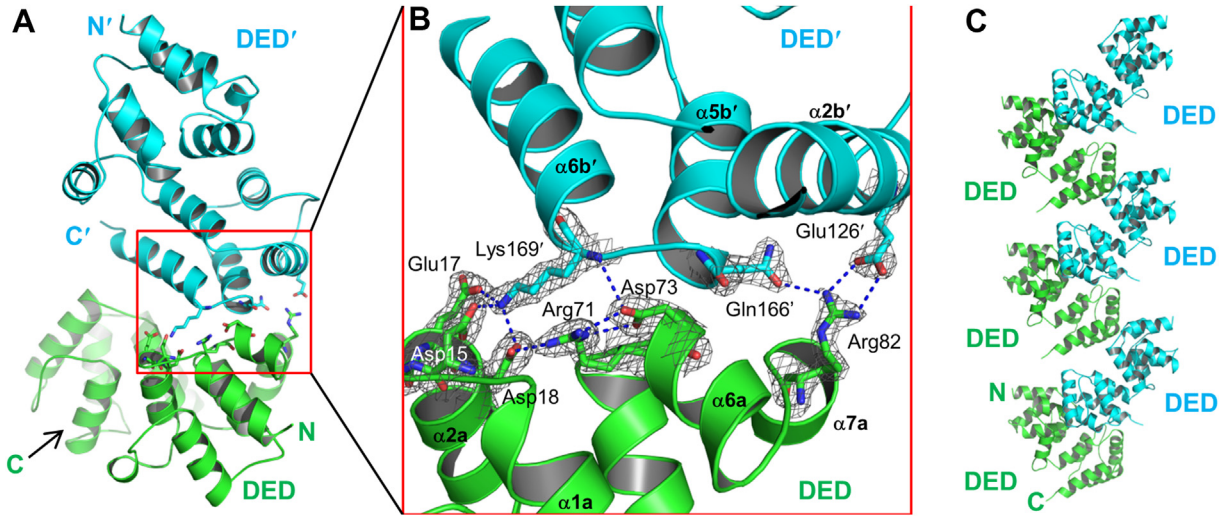

Fig. 4. Crystal packing of the DEDs of Casp8$^{F122A/I128D}$ in the crystal lattice. A) Structures of the DEDs of Casp8$^{F122A/I128D}$ in an asymmetric units, containing a dimer of the DEDs (DED and DED′). B) The intermolecular packing interface of the DEDs of Casp8$^{F122A/I128D}$ in the asymmetric unit. The key residues are shown in stick representation. 2Fo–Fc electron density maps for key residues are contoured at a level of 1.5σ. C) Potential filamentous structure formed by the continuingly packing DEDs of Casp8$^{F122A/I128D}$ mediated by the dimeric interface shown in A) and B).

Lys169 in DED2 of caspase-8 is replaced by a hydrophobic residue Leu167 in DED2 of MC159, which would impair the interfacial hydrogen bonding network and thus block the formation of death effector filament. This analysis is consistent with the fact that the tandem DEDs of MC159 cannot form death effector filaments [18,20,21].

Compared with the aggregating propensity of the DEDs of wild-type caspase-8, the mutations F122A and I128D markedly reduce the aggregation and improve the solubility, suggesting that Phe122 and Ile128 might involve in the self-assembly of the DEDs of caspase-8. However, these two residues are not involved in the described dimeric interface, indicating that they play the role in the self-assembly through other possible interfaces in physiological conditions. Moreover, gel filtration data only showed a single peak corresponding to the monomer for the purified DEDs of Casp8$^{F122A/I128D}$ (Fig. 1D). The determined dimeric structure thus might be the result of crystal packing in the high protein concentration during crystallization, or might just contribute to the formation of death effector filaments upon non-physiological overexpression of the DEDs of caspase-8 in cells.

Conflict of interest

There is no conflict of interest.

Acknowledgments

This work was supported by funds from the Ministry of Science and Technology 2012CB722602 (to J.M.Q.), 2013CB911501 (to T.W.); the NSFC 21290183 and 81373326 (to J.M.Q.), NSFC31300600 (to T.W.); Shenzhen government JCYJ20130331144947526 and GJHZ20120614144733420 (to J.M.Q.), KQCX20130627103353535 and GGJS20130329180714793 (to T.W).

Transparency document

The Transparency Document associated with this article can be found in the online version at http://dx.doi.org/10.1016/j.bbrc.2015.05.054.

References

[1] A. Oberst, D.R. Green, It cuts both ways: reconciling the dual roles of caspase 8 in cell death and survival, Nat. Rev. Mol. Cell Biol. 12 (2011) 757–763.
[2] G. Salvesen, C.M. Walsh, Functions of caspase-8: the identified and the mysterious, Semin. Immunol. 26 (2014) 246–252.
[3] M. Kruidering, G.I. Evan, Caspase-8 in apoptosis: the beginning of "The End"? IUBMB Life 50 (2000) 85–90.
[4] T.B. Kang, S.H. Yang, B. Toth, A. Kovalenko, D. Wallach, Caspase-8 blocks kinase RIPK3-mediated activation of the NLRP3 inflammasome, Immunity 38 (2013) 27–40.
[5] C. Guenther, E. Martini, N. Wittkopf, K. Amann, B. Weigmann, H. Neumann, M.J. Waldner, S.M. Hedrick, S. Tenzer, M.F. Neurath, C. Becker, Caspase-8 regulates TNF-α-induced epithelial necroptosis and terminal ileitis, Nature 477 (2011) 335–339.
[6] T. Bohgaki, J. Mozo, L. Salmena, E. Matysiak-Zablocki, M. Bohgaki, O. Sanchez, A. Strasser, A. Hakem, R. Hakem, Caspase-8 inactivation in T cells increases necroptosis and suppresses autoimmunity in Bim$^{-/-}$ mice, J. Cell Biol. 195 (2011) 277–291.
[7] J. Senft, B. Helfer, S.M. Frisch, Caspase-8 interacts with the p85 subunit of phosphatidylinositol 3-kinase to regulate cell adhesion and motility, Cancer Res. 67 (2007) 11505–11509.
[8] M. Muzio, A.M. Chinnaiyan, F.C. Kischkel, K. O'Rourke, A. Shevchenko, J. Ni, C. Scaffidi, J.D. Bretz, M. Zhang, R. Gentz, M. Mann, P.H. Krammer, M.E. Peter, V.M. Dixit, FLICE, a novel FADD-homologous ICE/CED-3-like protease, is recruited to the CD95(Fas/APO-1) death-inducing signaling complex, Cell 85 (1996) 817–827.
[9] N. Keller, J. Mares, O. Zerbe, M.G. Gruetter, Structural and biochemical studies on procaspase-8: new insights on initiator caspase activation, Structure 17 (2009) 438–448.
[10] J.W. Yu, P.D. Jeffery, Y. Shi, Mechanism of procaspase-8 activation by c-FLIP$_L$, Proc. Natl. Acad. Sci. U. S. A. 106 (2009) 8169–8174.
[11] H. Blanchard, L. Kodandapani, P.R.E. Mittl, S.D. Marco, J.F. Krebs, J.C. Wu, K.J. Tomaselli, M.G. Gruetter, The three-dimensional structure of caspase-8: an initiator enzyme in apoptosis, Structure 7 (1999) 1125–1133.
[12] J.W. Yu, Y. Shi, FLIP and the death effector domain family, Oncogene 27 (2008) 6216–6227.
[13] H.H. Park, Y.C. Lo, S.C. Lin, L.W. Wang, J.K. Yang, H. Wu, The death domain superfamily in intracellular signaling of apoptosis and inflammation, Annu. Rev. Immunol. 25 (2007) 561–586.
[14] C.H. Weber, C. Vincenz, The death domain superfamily: a tale of two interfaces? Trends Biochem. Sci. 26 (2001) 475–481.
[15] M.G. Valmiki, J.W. Ramos, Death effector domain-containing proteins, Cell. Mol. Life Sci. 66 (2009) 814–830.
[16] F.L. Scott, B. Stec, C. Pop, M.K. Dobaczewska, J.E.J. Lee, E. Monosov, H. Robinson, G.S. Salvesen, R. Schwarzenbacher, S.J. Riedl, Cytotoxicity-dependent APO-1 (Fas/CD95)-associated proteins form a death-inducing signaling complex (DISC) with the receptor, EMBO J. 14 (1995) 5579–5588.
[17] J.K. Yang, Death effector domain for the assembly of death-inducing signaling complex, Apoptosis 20 (2015) 235–239.
[18] R.M. Siegel, D.A. Martin, L.X. Zheng, S.Y. Ng, J. Bertin, J. Cohen, M.J. Lenardo, Death-effector filaments: novel cytoplasmic structures that recruit caspases and trigger apoptosis, J. Cell Biol. 141 (1998) 1243–1253.

[19] L.S. Dickens, R.S. Boyd, R. Jukes-Jones, M.A. Hughes, G.L. Robinson, L. Fairall, J.W.R. Schwabe, K. Cain, M. MacFarlane, A death effector domain chain DISC model reveals a crucial role for caspase-8 chain assembly in mediating apoptotic cell death, Mol. Cell 47 (2012) 291–305.
[20] J.K. Yang, L.W. Wang, L.X. Zheng, F.Y. Wan, M. Ahmed, M.J. Lenardo, H. Wu, Crystal structure of MC159 reveals molecular mechanism of DISC assembly and FLIP inhibition, Mol. Cell 20 (2005) 939–949.
[21] F.Y. Li, P.T. Jeffery, J.W. Yu, Y. Shi, Crystal structure of a viral FLIP: insights into flip-mediated inhibition of death receptor signaling, J. Biol. Chem. 281 (2006) 2960–2968.
[22] A.J. McCoy, R.W. Grosse-Kunstleve, P.D. Adams, M.D. Winn, L.C. Storoni, R.J. Read, Phaser crystallographic software, J. Appl. Crystallogr. 40 (2007) 658–674.
[23] P.D. Adams, P.V. Afonine, G. Bunkoczi, V.B. Chen, I.W. Davis, N. Echols, J.J. Headd, L.W. Hung, G.J. Kapral, R.W. Grosse-Kunstleve, A.J. McCoy, N.W. Moriarty, R. Oeffner, R.J. Read, D.C. Richardson, J.S. Richardson, T.C. Terwilliger, P.H. Zwart, PHENIX: a comprehensive python-based system for macromolecular structure solution, Acta Crystallogr. D. Biol. Crystallogr. 66 (2010) 213–221.
[24] P. Emsley, K. Cowtan, Coot: model-building tools for molecular graphics, Acta Crystallogr. D. Biol. Crystallogr. 60 (2004) 2126–2132.
[25] G.N. Murshudov, A.A. Vagin, E.J. Dodson, Refinement of macromolecular structures by the maximum-likelihood method, Acta Crystallogr. D. Biol. Crystallogr. 53 (1997) 240–255.
[26] M.D. Winn, C.C. Ballard, K.D. Cowtan, E.J. Dodson, P. Emsley, P.R. Evans, R.M. Keegan, E.B. Krissinel, A.G. Leslie, A. McCoy, S.J. McNicholas, G.N. Murshudov, N.S. Pannu, E.A. Potterton, H.R. Powell, R.J. Read, A. Vagin, K.S. Wilson, Overview of the CCP4 suite and current developments, Acta Crystallogr. D. Biol. Crystallogr. 67 (2011) 235–242.
[27] W.L. Delano, The PyMol Molecular Graphics System, Delano Scientific LLC, San Carlos, CA, USA, 2002. http://www.pymol.org/.
[28] M. Eberstadt, B. Huang, Z. Chen, R.P. Meadows, S.C. Nq, L. Zheng, M.J. Lenardo, S.W. Fesik, NMR structure and mutagenesis of the FADD (Mort1) death-effector domain, Nature 392 (1998) 941–945.
[29] P.E. Carrington, C. Sandu, Y.F. Wei, J.M. Yang, L. Hill, G. Morisawa, T. Huang, E. Gavathiotis, Y. Wei, M.H. Werner, The structure of FADD and its mode of interaction with procaspase-8, Mol. Cell 22 (2006) 599–610.
[30] J.R. Muppidi, A.A. Lobito, M. Ramaswamy, J.K. Yang, L. Wang, H. Wu, R.M. Siegel, Homotypic FADD interactions through a conserved RXDLL motif are required for death receptor-induced apoptosis, Cell Death Different. 13 (2006) 1–10.
[31] A.P. Minton, How can biochemical reactions within cells differ from those in test tube? J. Cell Sci. 119 (2006) 2863–2869.